

Local symmetries and order-disorder transitions in small macroscopic Wigner islandsGwennou Coupier,¹ Claudine Guthmann,¹ Yves Noat,² and Michel Saint Jean^{1,*}¹*Laboratoire Matière et Systèmes Complexes, Université Paris 7, Unité mixte du C.N.R.S 7057, 140 rue de Lourmel, 75015 Paris, France*²*Institut des NanoSciences de Paris, Universités Paris 6/Paris 7, Unité mixte du C.N.R.S 7588, 140 rue de Lourmel, 75015 Paris, France*

(Received 17 November 2004; published 5 April 2005)

The influence of local order on the disordering scenario of small Wigner islands is discussed. A first disordering step is put in evidence by the time correlation functions and is linked to individual excitations resulting in configuration transitions, which are very sensitive to the local symmetries. This is followed by two other transitions, corresponding to orthoradial and radial diffusion, for which both individual and collective excitations play a significant role. Finally, we show that, contrary to large systems, the focus that is commonly made on collective excitations for such small systems through the Lindemann criterion has to be made carefully in order to clearly identify the relative contributions in the whole disordering process.

DOI: 10.1103/PhysRevE.71.046105

PACS number(s): 64.60.Cn, 68.65.-k

I. INTRODUCTION

Many efforts have been intended in past years to understand properties of mesoscopic devices in which interacting particles are confined. For instance, these particles can be vortices in mesoscopic shaped superconductors [1,2], electrons in quantum dots [3], strongly coupled rf dusty plasma [4], trapped cooled ions [5], vortices in superfluid ⁴He [6], electron dimples on a liquid helium surface [7], vortices in a Bose-Einstein condensate [8], or colloidal particles [9]. More recently, in order to take advantage of the macroscopic scale to explore the properties of such systems, we have proposed a macroscopic system consisting of N interacting charged balls of millimetric size free to move on a plane conductor and confined electrostatically, the temperature being simulated by a mechanical shaking [10]. Using this system we observed the equilibrium configurations of the Wigner islands obtained for circular [11] and elliptic confinements [12].

Our previous study, essentially focused on static properties, conclude that at low temperature and for a circular confining potential, the observed small islands ($N < 40$) present self-organized patterns constituted by concentric shells in which the balls are located. As it was widely discussed in the literature [13–15], this peculiar structure is due to the competition between the ordering into a triangular lattice symmetry, which appears for infinite two-dimensional electrostatic systems, and the circular symmetry imposed by the confining potential. In the following, the Wigner islands will be described by the configuration $(N_0 - N_1 - N_2 - \dots)$ where N_i is the number of balls in the i th shell from the center.

Surprisingly, the influence of the thermal fluctuations on the phase behavior which was an important question largely studied for the two-dimensional extended systems has been little discussed in such small systems. The studies devoted to this question are essentially numerical and focused on the

temporal stabilities of the different configurations [16,17], their spectral properties [18,19] or the mean displacements of the particles [14]. Let us, however, indicate an interesting experimental work concerning the “melting” process of colloidal interacting particles islands [20,21]. “Melting” in two-dimensional quantum electron clusters has also been recently studied in Ref. [22].

Phase transitions in two-dimensional large crystals have mainly been described by the changes in the asymptotic behavior of spatial correlation functions. For instance, the Kosterlitz-Thouless-Halperin-Nelson-Young (KTHNY) theory predicts a two-step melting scenario according to which the liquid phase is reached when bond-orientational correlations become short-range [23,24]. Parallely, it has been suggested that temporal correlations should have the same behavior as the spatial ones [25]. This has recently been put in evidence experimentally for colloidal systems [9,26].

On the other hand, the previous studies on small interacting systems always refer to a generalization of the well-known Lindemann’s method employed to describe the order-disorder transition for large systems [27], which considers the liquid phase is reached when the mean square displacements relatively to the lattice parameter of the particles go beyond the value $\gamma_M = 0.1$ (which seems to be independent of the interaction [27,28]), or 0.05 for each coordinate. Note that it has been shown that, for infinite systems, the transition temperature exhibited there is the same as the one given by the correlation functions [29]. Let us underline that no such result is known for small systems.

For the latter, the studies lying on Lindemann’s criterion predict or observe that the shell-structured islands become less ordered while the temperature increases. They describe a two-step process corresponding to two different transition temperatures. At very low temperature, each particle is thermally excited in its local potential; a first transition appears at the temperature T_O when the orientational order between the shells is lost. This first transition is followed by a second one, at the temperature T_R , which corresponds to the emergence of the radial diffusion of particles between the shells,

*Electronic address: saintjean@gps.jussieu.fr

as well as an angular diffusion in the shells. For higher temperature, the initial order is completely destroyed. The transition temperatures T_O and T_R are, respectively, identified as the temperatures at which the intershell angular and radial mean square displacements have a rapid and strong increase [14].

In this paper, we discuss the influence of the local order on the “melting”. Indeed, for small islands, singular events such as a unique jump of only one particle from one shell to another one result to an important modification of the system since such an intershell jump corresponds to a transition between well-separated stable and metastable equilibrium configurations of different geometry. Consequently, such jumps will modify the bond-orientational correlation functions. We shall show that, for a given temperature, those configurations switches and thus the disordering process are controlled by the local geometry. In order to distinguish between those events and the collective excitations of the particles, we calculate the Lindemann parameters on each shell and for each configuration separately, without taking into account jumps between shells. We determine the temperatures at which the collective excitations appear and destroy the ordered configurations. This unusual Lindemann procedure is in agreement with our definition of an ordered system as a system always close to its most symmetrical configuration. For instance, an intershell jump which does not destroy the local symmetry does not have to be considered as relevant in our description. This will explain why the obtained critical temperatures will be higher than the one determined by the usual Lindemann method which includes all kind of displacements in the calculation of the parameters, as in Ref. [14]. Notice that this question is specific to small systems since in large systems there is a continuum of states and individual excitations are hidden by collective ones.

In order to evaluate the relative importance of these different contributions to the “melting”, we have experimentally observed the evolution of macroscopic Wigner crystals while the effective temperature is increased. To emphasize the contribution of the individual excitations with respect to the collective ones, we have selected a set of systems which have very different local symmetry for a similar number of balls in order to present different configuration transition behaviors for almost the same kind of collective excitations. We chose Wigner islands consisting in $N=18$, 19, and 20 interacting particles confined in a circular frame. These systems, in spite of a very close number of balls, are very different from the local symmetry point of view and the resulting excitation energy spectra. Indeed, the “magic number” system $N=19$ exhibits a threefold symmetry, as its ground configuration is (1-6-12). In fact, the latter shell can be divided into two subshells of 6 balls, as it was numerically shown in Ref. [13], however, the difference between the two radii being rapidly of the same order as the thermally induced radial fluctuations, we will still refer to this configuration as the (1-6-12) one. By contrast, the ground configurations of $N=18$ and $N=20$ systems are constituted by incommensurable shells (in the sense that the ratio between the number of balls on each shell is not an integer), their ground states being respectively (1-6-11) and (1-6-13). When the temperature increases, the two lower excited states of

each system can be reached. In spite of the radial displacements due to the temperature, the ringlike structure remains and the configurations can be very well identified.

- (i) For 18 balls: (1-6-11), (1-5-12), (0-6-12);
- (ii) For 19 balls: (1-6-12), (1-7-11), (1-5-13); and
- (iii) For 20 balls: (1-6-13), (1-7-12), (2-6-12).

We can notice that only one ball jump from a shell to another is necessary to induce a configuration switch.

These configurations correspond exactly to those computed in Ref. [13] for logarithmic interparticle interaction potential, strongly suggesting this kind of interaction between the balls, at least within the range of our experimental interparticle distance [11]. This conclusion has been confirmed later by comparing the ground configuration obtained for elliptic confinement with the configuration of vortices calculated in similar shaped mesoscopic superconductors for which the intervortices interaction is logarithmic in the considered range of interparticle distance [12,30]. From the energetic point of view, the local symmetry differences between the various systems induce strong differences in their excitation energy spectra [13]. The configuration energies for $N=19$ and $N=18$ are well separated, however, the gap between the ground and the first excited state is larger for the magic number system. By contrast, the latter is very small for $N=20$.

In Sec. II, we present the experiments which validate the mechanical shaking as an effective thermodynamic temperature and we describe the parameters used to characterize the disorder, the configuration transitions and the collective excitations. The evolutions with temperature of these parameters for $N=18$, 19, and 20 islands will be described and discussed in details in Sec. III. In Sec. IV, the respective influence on the disordering of the individual and collective excitations will be discussed. We will show that, according to the considered parameter, different transition temperatures can be identified. In particular, the systems present an important configuration transition activity inducing disorder at a temperature smaller than those characterized by the Lindemann criterion. The melting will have to be considered rather as a disordering than a real melting.

II. EXPERIMENTAL PROCEDURES AND CHARACTERIZATION PARAMETERS

Our Wigner islands are constituted by millimetric stainless steel balls (of diameter $d=0.8$ mm and weight $m=2.15$ mg) located on the bottom electrode of a horizontal plane capacitor (a doped silicon wafer whereas the top electrode is a transparent conducting glass). An isolated metallic circular frame of diameter $D=10$ mm and height $h=1.5$ mm intercalated between the two electrodes confines the balls [11]. When a potential V is applied to the top electrode (the bottom one and the frame being linked to the ground), the balls become monodispersely charged, repel each other, and spread throughout the whole available space. For the currently used potential V (around a few hundred of volts), the charge of each ball has been evaluated to about 10^9 electrons. The whole cell is fixed on a plate linked with two independent loudspeakers supplied by a white noise

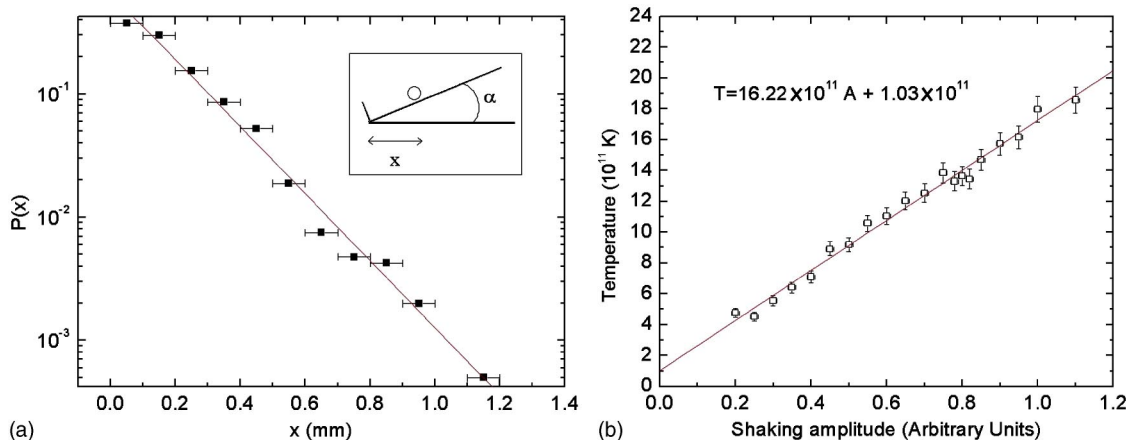


FIG. 1. Temperature calibration: (a) x position distribution for a trapped ball moving on an inclined plane (inset) and submitted to mechanical shaking (log scale). The good fit with Boltzmann law validates the mechanical shaking as an effective temperature. (b) Calibration of the effective temperature.

voltage. As we shall show later, this horizontal shaking results in an erratic movement of the balls which simulates an effective temperature that can be modified by tuning the shaking amplitude. In the experiment presented here, the system is always prepared in its ground configuration at low effective temperature and the temperature is progressively increased.

Throughout the experiment, images of the arrays of balls are recorded in real-time using a charge coupled device (CCD) camera, and their center of mass is detected. For each temperature, the positions of each ball are followed during 400 s, the minimum time between two snapshots being 100 ms. The characteristic time of the oscillation of a single ball in its local potential is, at low temperature, about half a second. Then, the choice of the total experiment time and the time interval allow us to track the balls (at least in the considered temperature range) and get statistically relevant data. The different configurations reached are then determined by counting the number of balls in each shell. In this procedure the radial limits of a shell are defined as the mean values between its radius and its neighbor's one, that have been measured in the ground state. They are independent from the temperature.

A. Temperature calibration

Before studying the “melting” of such systems, strong attention has been paid to show that the cell shaking effectively results in a brownian motion of the balls allowing the identification of this shaking with an effective temperature. We present here the experiments performed in order to calibrate this effective temperature and the “*in situ*” thermometer we have developed.

As in Ref. [31], we used a system for which the energy is well known: the calibration was obtained by the use of a single ball rolling on the silicon wafer which has been winded with an angle $\alpha=25^\circ$ from the horizontal plane. The ball can elastically bounce on a bottom wall. No electrostatic force is at stake and the only energy is the gravitational potential. For each voltage A applied on the loudspeakers, the

horizontal distances x of the ball center from the bottom wall have been measured through the capture of a few thousand snapshots of the ball. The recorded random x positions are distributed following the density $P(x)$.

In order to compare this density with the Boltzmann theory, it was fitted with the function

$$P(x) = \frac{mg \tan \alpha}{k_B T} e^{-E(x)/k_B T},$$

where $E(x)=mgx \tan \alpha$ is the potential energy of the ball and T the fit parameter which corresponds to the expected effective temperature, k_B being the Boltzmann constant.

Figure 1(a) presents the experimental data obtained for the voltage amplitude $A=1.0$ a.u. and the corresponding fit. At evidence Boltzmann law is obeyed. This very good agreement being observed whatever the voltages A , we may conclude that the mechanical shaking corresponds to an effective temperature. This effective temperature is obtained thanks to the fitting analysis, or more simply through the relationship $T=mg \langle x \rangle \tan \alpha/k_B$ and a calibration curve $T(A)$ has then been obtained. As shown in Fig. 1(b), the relation between A and T is affine within the range required to study the “melting”. Let us indicate that the temperature range is about 10^{11} K, which has no other signification than the energy range.

Finally, we have used this calibration to develop an *in situ* thermometer which is constituted by a single ball trapped in a second circular frame located near the main one and submitted to the same voltage. The effective temperature is determined by measuring the radial mean square displacement $\langle r^2 \rangle$ of this unique ball for each given shaking amplitude A and by identifying this displacement with the temperature $T(A)$ previously determined by the calibration procedure. Whatever the various thermometer diameters tested in order to optimize the sensibility of this thermometer ($D=5,6,7,8$, and 10 mm) and the applied potential V ($V=700,800,900,1000$ V) the mean square displacement $\langle r^2 \rangle$ varies linearly with the temperature. The same linearity is observed for the mean square speed. Figure 2 presents the

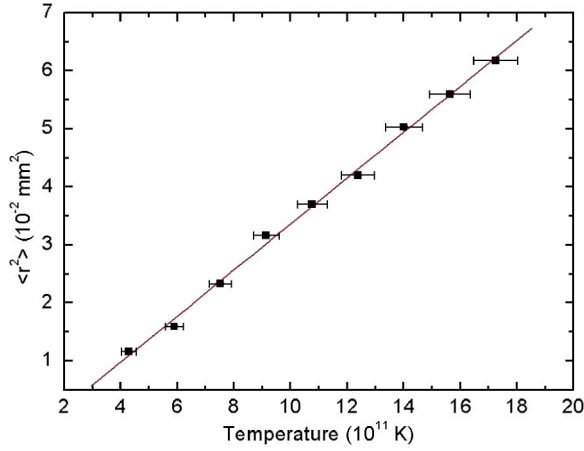


FIG. 2. Mean square displacement $\langle r^2 \rangle$ of the ball plotted vs temperature for $D=6$ mm and $V=900$ V.

variation $\langle r^2 \rangle (T)$ corresponding to the potential $V=900$ V and the retained diameter $D=6$ mm. This thermometer will give a precise determination of the temperature for any experiment to come, independently from the variations associated to the total weight of the support or to the loudspeakers' aging.

B. Correlation functions

The bond-orientational correlation function $g_6(t)$ is relevant in order to characterize phase transitions in two-dimensional systems. It is defined by

$$g_6(t) = |\langle e^{i6[\theta(t+t_0) - \theta(t_0)]} \rangle|,$$

where $\theta(t)$ is the angle of a fixed bond between two particles and $\langle \rangle$ denotes an averaging over all bonds. In infinite two-dimensional systems, g_6 tends to a constant roughly equal to 1 at low temperature. The system is then like an ordered crystal. If the temperature is higher than a temperature T_l , a strong decay with time is observed, which denotes a liquid phase.

Such a dynamical criterion offers experimental facilities since it is often easier to have long time acquisition rather than to observe a large sample of particles. In particular, we can readily use this criterion to characterize order-disorder transitions in small systems.

Note that the factor 6 in the exponential is adapted for hexagonal lattices, therefore we can expect the limit value at low temperature to be lower than 1 for our small systems in which the threefold symmetry is broken. On the other hand, the averaging being made only on $N(N-1)/2$ links, we cannot expect g_6 to go until zero value in the liquid phase, even at large time. These points apart, this parameter still measures the correlations and we can expect to measure the same global behaviors according to the temperature.

C. Configurations transition parameters

Two parameters easy to get experimentally have been identified in order to characterize the configuration transitions. The first of them is the jump rate R_J :

$$R_J = \lim_{t \rightarrow \infty} \frac{N_J(t)}{t},$$

where $N_J(t)$ is the total number of configuration switches during the period t . This parameter is an indicator of the "transition activity" of the system. Qualitatively, this parameter is small at low temperature when only a few transitions occurs and increases strongly with temperature when energetical barriers can be overcome.

A second way to characterize more quantitatively the transition rate is to measure the mean time required to escape from each state or the mean residence time in each state. Let us consider for instance a Wigner island at low temperature; this system can be understood as a two level system characterized by a ground state E_g and one metastable state E_m (the only one that is reachable if the temperature is sufficiently low). The thermal fluctuations induce transitions between those two configurations. These transitions in the real space can be mapped in the phase space by the jump of a fictive particle from a well to another, characterized by their depth E_g and E_m and a saddle point E_s .

Under the assumption that all escape attempts are independent and of weak probability, the probability for the particle to stay in a state of energy E during a time τ is:

$$P(\tau) = \frac{1}{\tau_0} e^{-\tau/\tau_0},$$

where $\tau_0 = \langle \tau \rangle$ is the mean residence or Kramers time. It depends on the energy barrier and on the temperature and is given by [32]:

$$\langle \tau \rangle = \tau_r e^{(E_s - E)/k_B T},$$

where $E_s - E$ is the barrier energy, and τ_r is the relaxation time within the well.

The energetical barriers can be measured by the slope of the curve describing the variations of the mean residence times in log scale as a function of $1/T$. Similarly, the spectrum of the excitation energies is determined through the ratio of mean residence times in the two wells.

Qualitatively, this analysis can be extended to the case of high temperature for which the system explores more than the two first levels and reaches higher excited levels. But the possibility for a particle to escape a well in different ways whose relative weight should depends on the geometry leads to a more acute problem.

We have tested the validity of this analysis in the case of the two-level systems $N=5$ and $N=6$. These two cases are interesting since they involve in their respective configuration transitions the two kinds of individual jump observed in the Wigner excitations. For $N=5$, the ground configuration consists in a unique shell (5) whereas the metastable configuration (1-4) requires a centripetal displacement of a ball. By contrast, the $N=6$ ground state is a centered configuration (1-5) and the metastable configuration (6) is reached after a centrifugal displacement of ball.

In Fig. 3 we present the variation with the temperature of the ratio $\langle \tau_{centered} \rangle / \langle \tau_{circle} \rangle$, where $\tau_{centered}$ stands for the residence time in the centered configuration, respectively (1-4)

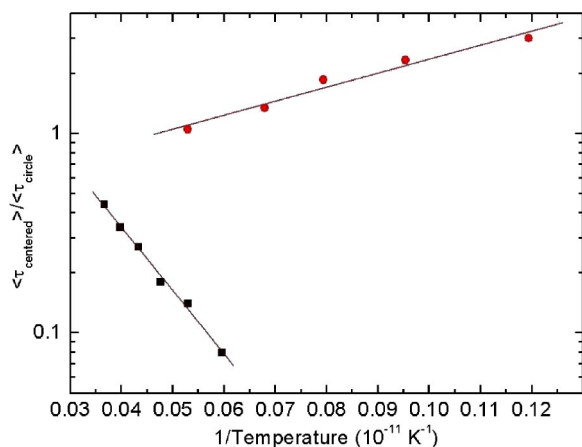


FIG. 3. Evolution with the temperature of the residence mean times ratio for two-level systems: five balls (■) and six balls (●). Ratios are in log scale. Note the signs of the slopes that prove that (5) and (1–5) are the ground states for the five-ball and six-ball systems, respectively.

or (1–5), and τ_{circle} denotes the residence time in the one-shell configuration, respectively, (5) or (6). For the two selected systems these variations obey Kramers' relation.

According to this Boltzmannian description, we will characterize in the following the configurations transitions by R_j and by the mean residence times in each configuration. These parameters depend on the configuration energy spectra and thus, are extremely sensitive to the local symmetry of the configurations.

D. Lindemann-like criterion

In order to explore the collective excitations of Wigner islands through a Lindemann criterion, the mean square deviations of the balls from their equilibrium locations have to be calculated.

For three-shell configurations and circular symmetry [14], we have to calculate, for each configuration and for shells 1 and 2, the radial displacements

$$u_r^2 = \frac{1}{N_s} \sum_{i=1}^{N_s} (\langle r_i^2 \rangle - \langle r_i \rangle^2) / r_0^2,$$

the relative angular intrashell displacements

$$u_{\theta 1}^2 = \frac{1}{N_s} \sum_{i=1}^{N_s} (\langle (\theta_i - \theta_{i_1})^2 \rangle - \langle \theta_i - \theta_{i_1} \rangle^2) / \theta_0^2,$$

and, for each configuration and for shell 1, the relative angular intershell displacements

$$u_{\theta 2}^2 = \frac{1}{N_s} \sum_{i=1}^{N_s} (\langle (\theta_i - \theta_{i_2})^2 \rangle - \langle \theta_i - \theta_{i_2} \rangle^2) / \theta_0^2,$$

where (r_i, θ_i) are the polar coordinates of a ball with respect to the center of the confining frame, i_1 indicates the right neighbor of the ball i , and i_2 indicates its nearest neighbor in the surrounding shell, which is determined every snapshot.

$r_0 = 1/\sqrt{\pi n}$, where n is the balls density, is the mean radial free space for a ball and $\theta_0 = 2\pi/N_s$ is the mean interball angular distance in the shell consisting in N_s balls. $\langle \rangle$ indicates an average over time.

These deviations are relative displacements (with respect to another ball or the center of the system), therefore they are relevant in order to exhibit a Lindemann-like criterion comparable to the one used for larger two-dimensional systems [27]. However, we will not be able to discuss as in the latter paper about the values of the dimensionless parameter $\Gamma = E/k_B T$, where E is a typical interaction energy between two particles, since we do not have numerical values for the potential energies in our system at the present time.

Note that we have discriminated between the different configurations. This is allowed since the radial displacements, as we shall show, are around a sixth of the distance between the two shells whatever the effective temperature, then the shells are always well identified. This choice is motivated by our requirements of precise information about the influence of the local order on the “melting”. The temperature dependencies of the displacements averaged over all the configurations have also been calculated. This procedure is not the same as the one used in Ref. [14], where the distinction between shells is only made at the beginning of the numerical simulation, so we shall expect lower values for our radial displacements that do not include intershell jumps.

III. IDENTIFICATION OF TRANSITION TEMPERATURES

A. Bond-orientational decorrelations

In Figs. 4(a)–4(c) we present typical time correlation functions $g_6(t)$ for five different temperatures and for the three systems, for which the same behaviors are observed: at low temperature, a constant value is reached, indicating an ordered state. At higher temperature, the correlations decay strongly. As in large systems, we can define a “melting” temperature $T_l(N)$. We notice that the $N=19$ system keeps an ordered structure denoted by a quasicontant correlation function until a much higher temperature than the two other systems. Indeed, the transition temperatures $T_l(N)$ are sensitively different according to the number of balls N : $T_l(18)$ is less than 13×10^{11} K, whereas $T_l(19)$ is more than 18×10^{11} K and $T_l(20)$ between both. Note our goal is not to measure precise transition temperatures, but to put in evidence the mechanisms involved in the disordering. As we shall see, the different transition temperatures are sufficiently separated to do such an analysis. In the following, we will then investigate the two expected mechanisms for this disordering: configuration transitions and collective excitations through Lindemann criterion.

B. Configurations transitions

The first indication of the configuration transition activity can be evidenced by observing the evolution of the jump rate R_j while the effective temperature increases. These variations are shown in Fig. 4(d) for the different studied systems.

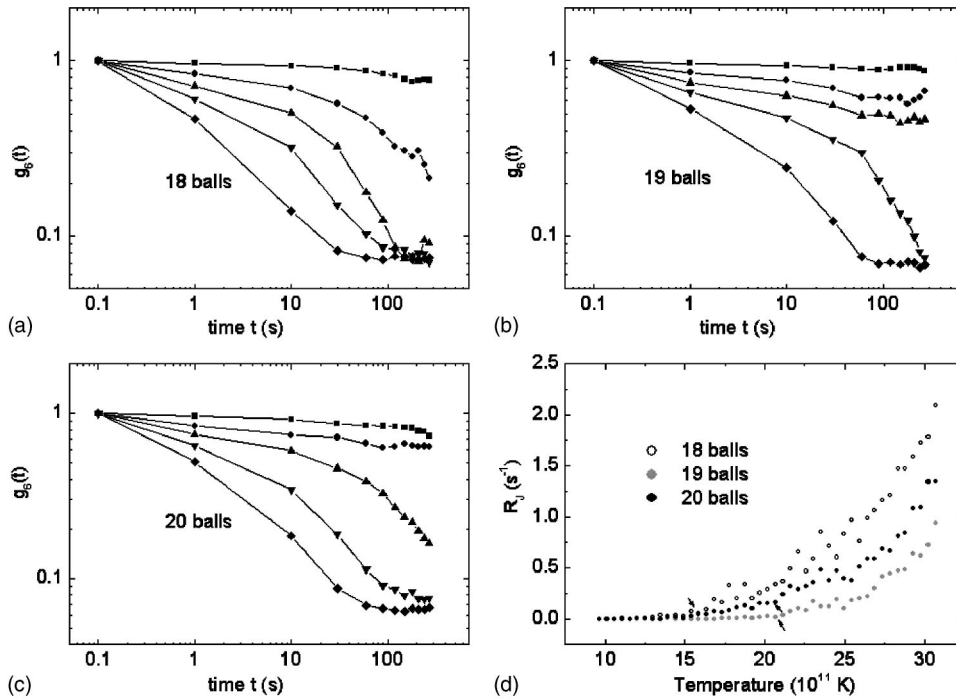


FIG. 4. Variations of orientational correlation function and jump rate with temperature. Bond-orientational time correlation function for five temperatures: (■) $T=9.6 \times 10^{11}$ K, (●) $T=13.0 \times 10^{11}$ K, (▲) $T=17.8 \times 10^{11}$ K, (▼) $T=23.0 \times 10^{11}$ K, (◆) $T=30.2 \times 10^{11}$ K; (a) $N=18$, (b) $N=19$, and (c) $N=20$. (d) Jump rate vs temperature. Arrows show the temperature at which the second excited state is reached.

Whatever the number of balls, R_J presents the same qualitative behavior: it is close to zero at low temperature and increases strongly at higher temperature. These variations correspond to a progressive augmentation of the number of transitions activated at the effective temperature. Whatever the temperature, the smallest jump rate is associated to $N=19$ system and the one associated to $N=20$ is always smaller than the one corresponding to $N=18$. In order to describe more quantitatively these behaviors and their differences, let us introduce transition temperatures which characterize the “beginning” of the R_J increases. We have chosen to name transition temperature the temperature at which the ground configuration begin to switch. Let us nevertheless indicate that this transition temperatures does not correspond to an actual sudden transition since the jump rate R_J rises progressively. Note that experimentally, the infinite time limit in the R_J definition corresponds to the maximum measurement time and its finite value could alter the R_J value. However, a complete analysis has shown that the variation with temperature of R_J is independent from this experimental limit provided that this limit was largely higher than the mean residence time of the system in each configuration. In our experiments we chose $t_{max}=400$ s which satisfied this condition.

The analysis of the evolution of the residence times distribution shows that, for $N=19$, the transition temperature $T_J(19)$ is 20×10^{11} K, much higher than the temperatures $T_J(18)$ and $T_J(20)$ which are, respectively, 14×10^{11} K and 17×10^{11} K. At larger temperature, the second excited states are reached. The corresponding temperatures are, respectively, 21×10^{11} K, 16×10^{11} K, and 21×10^{11} K for $N=19$, 18, and 20 and are indicated by arrows in Fig. 4(d). Those temperatures might correspond to the critical temperatures given in Ref. [16] where the rate of radial jumps is calculated. This is exactly the same parameter as our jump rate

since each configuration switch involves only one ball jump from one shell to another.

These behavior differences between the systems are still more obvious when we study their mean residence times in the ground state. In Fig. 5 we have plotted the logarithm of these times $\langle \tau \rangle$ versus the inverse of the effective temperature. We obtain a linear variation, which is in agreement with the Boltzmann law description presented earlier, the curves slopes being equal to the barrier heights for escaping the configuration. We can observe that these slopes are different according to the number of balls. The highest slope is associated to the ground state $N=19$ and is equal to 192×10^{11} K, those corresponding to $N=18$ and 20 being respectively equal to 99×10^{11} K and 107×10^{11} K. This indicates that the ground state for $N=19$ is much more stable than the ground states associated to $N=18$ and 20, whose barrier

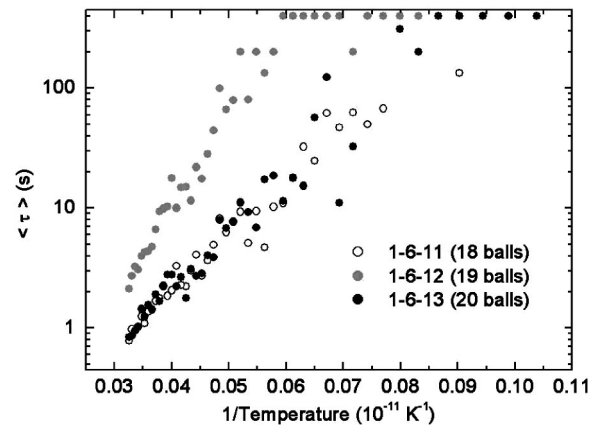


FIG. 5. Evolution with the temperature of the residence mean times in the ground state (the 400 s limit corresponds to the recording time but it is actually infinite). Times are in log scale.

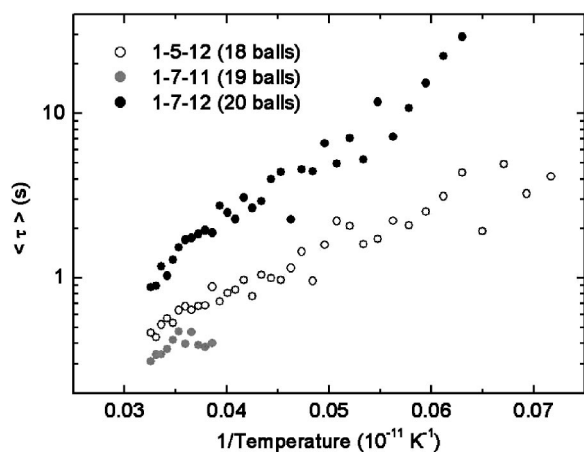


FIG. 6. Evolution with the temperature of the residence mean times in the first excited state. Times are in log scale.

heights are very similar since their corresponding slopes are roughly identical.

This analysis can be completed by studying the excited states (Fig. 6). The slopes for $N=18$ is 64×10^{11} K and is equal to 101×10^{11} K for $N=19$; in both systems, this suggests that the barrier is much lower than the ground state's one. On the contrary, the slope associated to the first excited state of $N=20$ is equal to 96×10^{11} K, almost the same as the barrier for the ground state. All these results are in good agreement with the energy levels calculated in Ref. [13]. Let us indicate that even when they are reachable, the other excited states are not easy to study since their higher energy involves too small statistical occurrences. Finally, these measurements allow us to determine the first excitation energy associated to each system. These energies are 35×10^{11} K, 91×10^{11} K, 11×10^{11} K, respectively, for $N=18, 19, 20$.

These measurements show that the “magic number” system corresponds to the deeper ground state and confirms its strong stability in comparison with the two other systems. As expected, the commensurability influences strongly the depth of the well, and consequently the transition temperature in R_J .

Let us conclude this section by indicating that obviously the jump rate R_J is related to the mean residence times. For instance, for a two-level system, R_J is simply equal to $2/(\langle \tau_1 \rangle + \langle \tau_2 \rangle)$, where subscripts 1 and 2 stand for the two levels. This relation is satisfied and confirms the self consistency of our results, at least up to a temperature at which a third level is reached.

C. Mean square displacements

We now turn to the study of the “melting” through Lindemann-like criterion. We will successively present the radial, intrashell and intershell mean square displacements averaged over all the configurations. In order to explore more precisely the relation between the local order and these collective parameters, we have compared them to the corresponding parameters before averaging. We shall show in particular that the procedure of averaging over the configurations, commonly used in literature, mask actually subtle

effects resulting from the configurations transitions, even though they do not infer that much on transition temperatures.

1. Radial displacements

The temperature dependencies of the radial mean displacements averaged over all the configurations are presented for the three different numbers of balls in Fig. 7(a).

The displacements corresponding to the inner shell (shell 1) present similar behaviors for the three systems. They vary regularly from 0.005 at low temperature and go on increasing until 0.05 at the highest experimental temperature, the highest and the lowest radial displacements being respectively associated to the systems $N=20$ and $N=19$, whatever the temperature. In this experimental temperature range, the low values of u_r^2 , smaller than the Lindemann criterion, indicate that each shell remains very well identified and that we can always discuss qualitatively the results in terms of shell entities. Notice that the highest obtained temperature corresponds to the ball-tracking limit, but we could forecast that the value would increase strongly beyond 0.05 after this temperature limit, since this value is far from being the maximal possible value, even though jumps from one shell to another are not taken into account. From this point of view, we can consider the highest experimental temperature is very close to the radial transition temperature transition T_R of these systems. The radial displacements of the outer shell (shell 2) are qualitatively similar to those observed for the shell 1 although their values are smaller and vary from 0.005 until 0.03. This can be explained by the fact that this shell is submitted to a regular and constant potential resulting from the confinement frame whereas shell 1 is submitted to fluctuant potential from both sides [14].

We have seen that geometrical considerations are responsible for the different configuration transition rates observed. It is therefore natural to examine if it is the same for the displacements. The radial mean displacements for the different configurations of the different systems are presented in Fig. 8. Notice that data for the excited states with low residence time present higher statistical error due to the smaller number of their occurrences; this is the case for instance for the second excited state for 18 and 20 balls and for both excited states for 19 balls.

As for the averaged curves, the radial displacements in the two shells of the systems in their ground configurations present regular increases with temperature. More precisely, for shell 1, we can observe that the $N=19$ (1-6-12) and $N=20$ (1-6-13) curves are identical whereas the displacement corresponding to $N=18$ (1-6-11) is higher whatever the temperature. For shell 2 the displacements are identical for $N=18$ (1-6-11) and $N=19$ (1-6-12) whereas those associated to $N=20$ (1-6-13) presents a higher value. The temperature dependencies observed for the excited states look like those associated to the ground states, with a constant switch. The highest u_r^2 values are now observed for $N=20$ (1-7-12) in the case of the shell 1 and for $N=18$ (1-5-12) in the case of the shell 2.

We cannot define a precise rule to explain the different behaviors. It seems, however, that, for a given temperature,

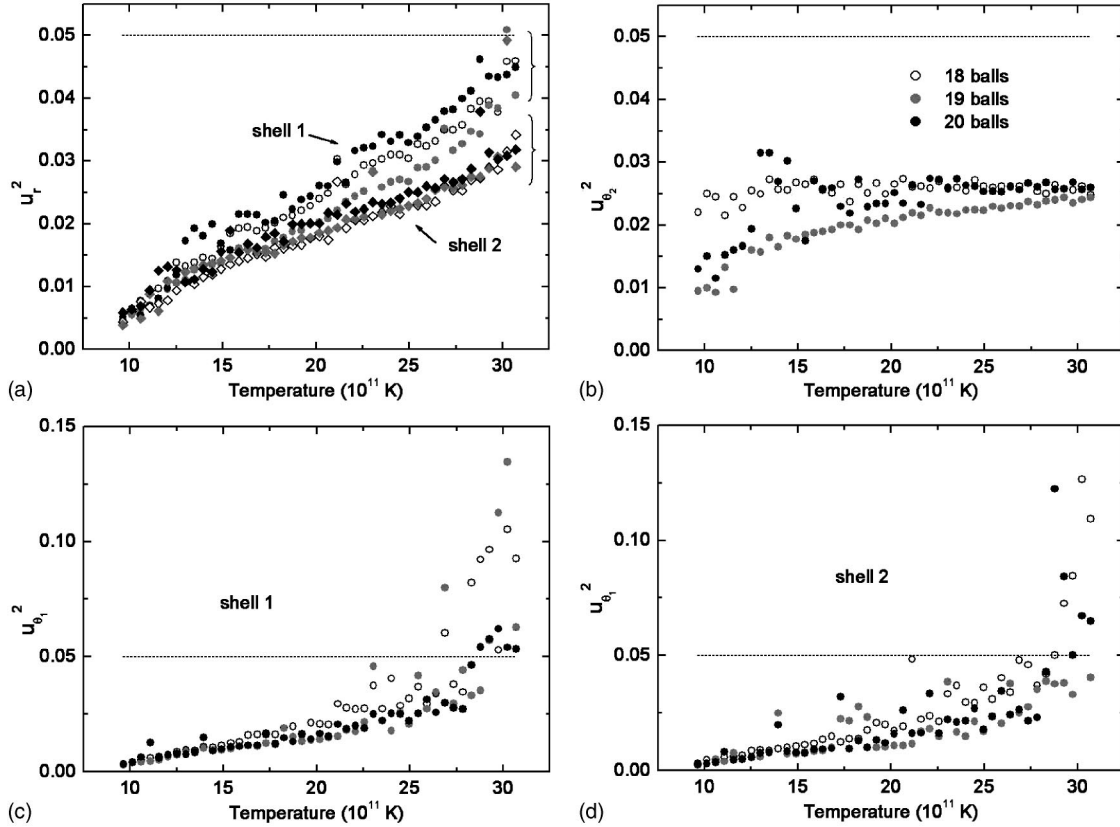


FIG. 7. Mean square displacements averaged over the three configurations versus temperature: (a) radial displacements u_r^2 for both shells, (b) intershell angular displacements $u_{\theta_2}^2$, (c) intrashell angular displacements $u_{\theta_1}^2$ in shell 1, and (d) intrashell angular displacements $u_{\theta_1}^2$ in shell 2.

the more balls in the shell, the larger the radial displacements. In the case of equality [that is to say, for the first shell, the couples (1-6-11),(0-6-12) and (1-6-13),(2-6-12) and for the second shell the couples (1-5-12),(0-6-12) and (1-7-12),(2-6-12)], we observe that the commensurable states have lower radial displacements. Those differences are higher than a possible distortion due to a renormalization by a different N_s .

The first statement can be simply understood by the fact that orthoradially squeezed balls have more kinetic energy to involve in their radial movement. In the case of a commensurable state, all the balls (for the first shell) or half of them (for the second shell) find themselves in front of a repelling ball of the other shell, which restrains their radial fluctuations. Note this result is opposite to what was reported for quantum dots in Ref. [22]: the authors exhibit higher radial displacements for magic number $N=19$.

Beyond these specific results, the comparison between the averaged and nonaveraged radial displacements show that even if some differences can be exhibited concerning their precise and relative values, global behavior remains the same: each shell will radially melt at the same temperature whatever the configuration.

2. Intrashell angular displacements

In the case of the angular mean displacements, the averaging does not introduce any distortion in the analysis, as it

can be seen in Fig. 9. So we will only discuss the mean displacements averaged over the configurations [Figs. 7(c) and 7(d)]. Like the radial displacements, the intrashell orthoradial displacements associated with the inner shell of ground configurations increase with the temperature. However, whereas the former keep on rising slowly, the angular ones begin to vary linearly and change very rapidly at almost the same temperature whatever the number of balls. By contrast, this similarity of behaviors is not observed for the outer shell: whereas the intrashell orthoradial displacements are identical for $N=18$ and $N=20$, in the case $N=19$, it remains smaller than 0.005 and without rapid rise.

The changes are observed when the displacements reach the critical value 0.05 in accordance with the Lindemann criterion. Thus, we can define from these data a transition temperature T_O or, rather, a temperature interval centered temperature on T_O (between 28×10^{11} K and 30×10^{11} K) after which intrashell orientational order is lost in a given configuration for $N=18$ and $N=20$. We can expect that the corresponding temperature is not far from the experimental limit in the case of $N=19$ since the balls in the shell 1 have begun to be non-correlated whereas the shell 2 is still rigid.

3. Intershell angular displacements

Let us now consider the intershell relative displacements which measures the ability of the two shells to find a stable position one with respect to the other. Their variations with

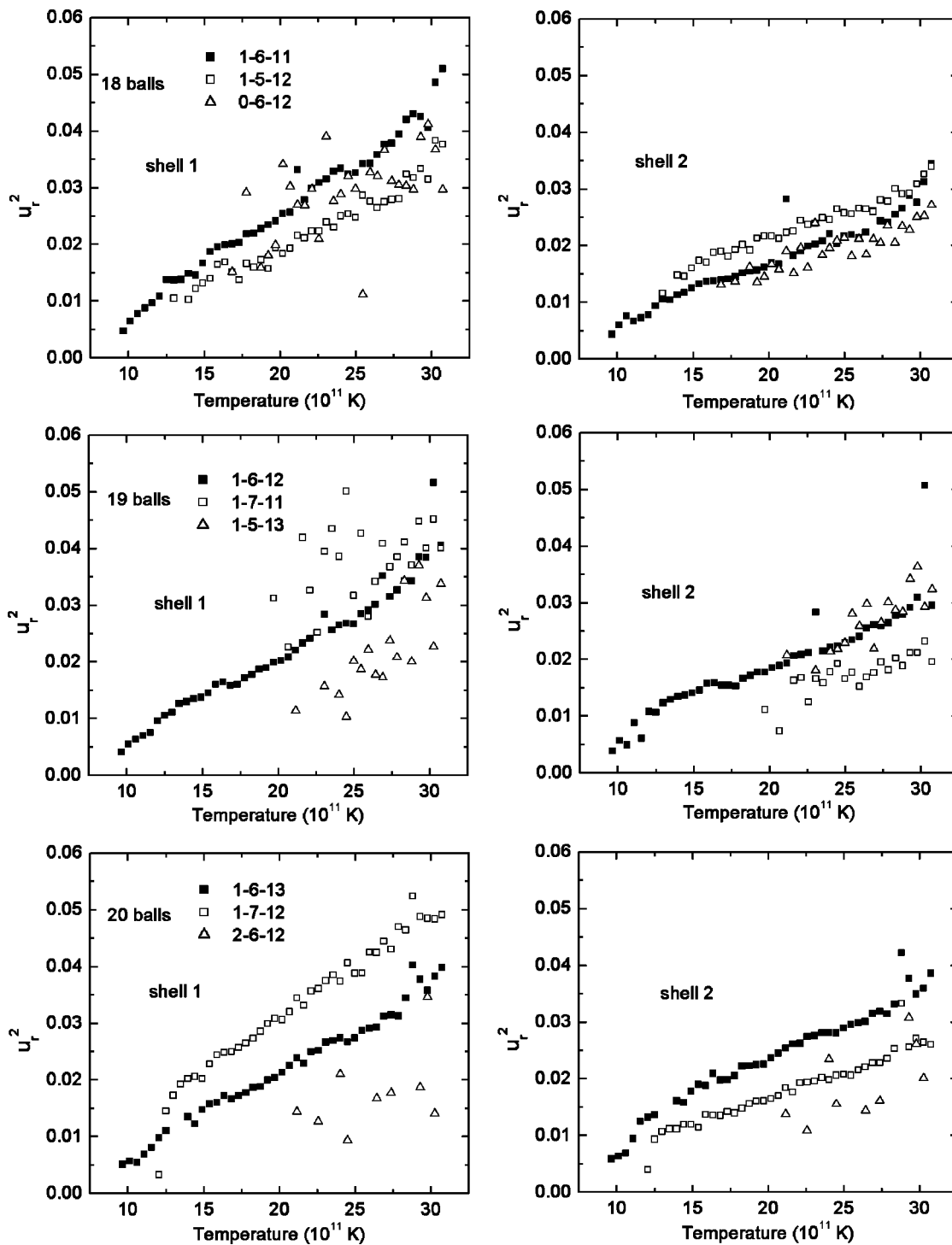


FIG. 8. Radial mean square displacements u_r^2 for the three systems and all configurations vs temperature.

temperature averaged over configurations are presented in Fig. 7(b) for the three systems. We can notice that even at low temperature these displacements are high and until $T \approx 18 \times 10^{11}$ K, the intershell angular displacements are larger than the corresponding intrashell and radial displacements. This indicates that at low temperature these intershell movements are the main effects resulting from the thermal fluctuations. Moreover, this temperature being smaller than T_O and T_R , we are allowed to discuss these results in terms of

well defined rigid shells in which the balls are regularly spaced.

At large temperature, $T > 18 \times 10^{11}$ K, the intershell angular displacements reach the same finite value whatever the system, this value being in fact its theoretical maximum. In this temperature range, the thermal energy is sufficient to overcome the barrier energies, which correlate the inner and outer shells. Since disorder is characterized by a deviation of the whole island from the symmetrical situation, note that the

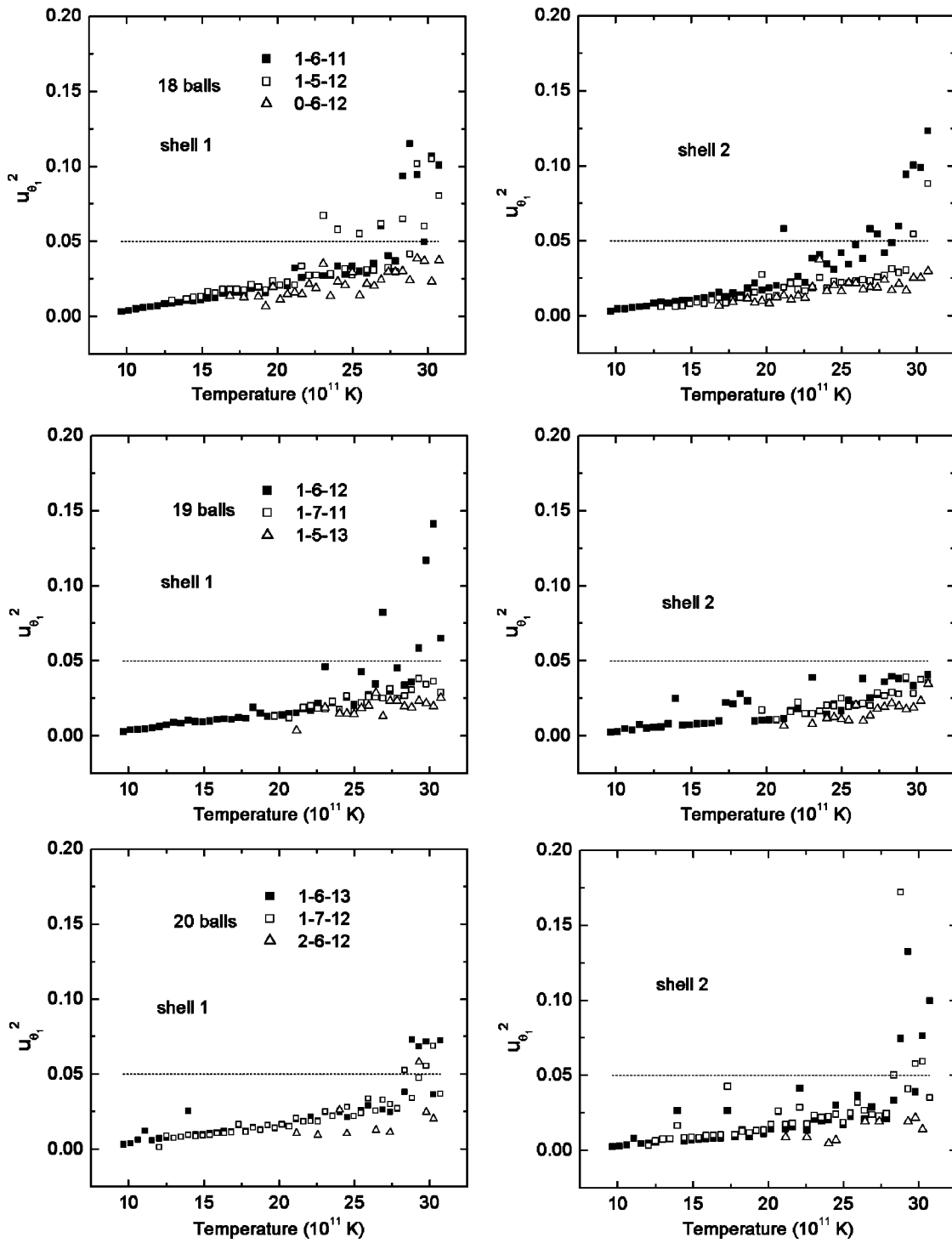


FIG. 9. Intrashell mean square displacements $u_{\theta_1}^2$ for the three systems and all configurations vs temperature.

intershell displacements are calculated considering the nearest neighbor at each time step, in order to take into account the invariance towards some rotations. Consequently, we will always have a small maximum value and will never observe a steep rise as in Ref. [14].

Below this temperature, a temperature range in which the effect of the local order has an essential play is well exhibited. In this temperature domain, the systems are mainly in

their ground state and the intershell angular displacement is lower for 19 balls than for 18 and 20 balls, the latter remaining of the same order. This can be simply explained by commensurability arguments: let us consider the shells as rigid rings; in the 1-6-12 configuration, shell 1 is submitted to a $2\pi/12$ periodic potential due to shell 2, then each of its balls can find itself in a potential well. On the contrary, in any other configuration uncommensurability implies that, if rigid,

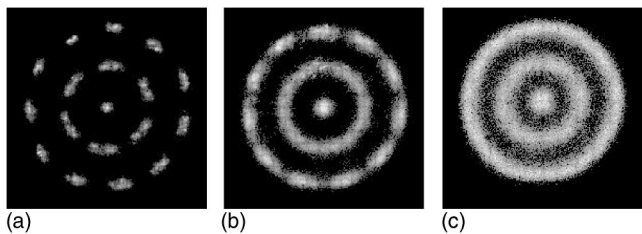


FIG. 10. Mean crystals for (a) $T < T_I$, (b) $T_O < T < T_R$, and (c) $T \sim T_R$.

the two shells cannot find a position for which every ball will be located in a minimum of energy, hence a higher instability.

IV. DISORDERING SCENARIO

The study of the transition temperatures T_I through correlation functions show that they depend strongly on the local order. Indeed, those temperatures are very different for the three systems, the $N=19$ magic system being more stable. As for temperatures around T_I , the systems can still be seen as sets of shells, comparison can be made between the temperatures T_I and the temperatures T_J of first configuration transition. Since they are very similar, we can infer that configuration transitions play an important role in the disordering, at least for intermediate temperatures. It can be simply understood by the fact that the islands are invariant by many rotations whatever the configuration, then a cycle of configuration transitions can induce disorder (from the correlation point of view), since the initial particles positions are not necessary recovered at the end of the transition cycle. Moreover, a configuration switch implies a complete reorganization in the shells. This disorder mechanism involving only one particle jump cannot be evidenced by the global parameters as the mean displacements used in the Lindemann approach. Note that even at low temperature, the orientational order between adjacent shells is already lost while their internal order is conserved; this suggests that the trajectory of the jumping particle might be not only radial but also orthoradial, taking advantage of the relative rotation of the two implied shells. This is also in accordance with the fact that commensurability considerations play a role for the intershell rotations as well as for the height of the energetical barriers. On the other hand, mere intershell rotation is not sufficient to induce disorder as defined by the correlation function, since the system will periodically find itself in the same position as the initial one.

If we focus now on collective displacements, a first transition occurs at the temperature $T_O > T_I$, which corresponds to the emergence of the angular intrashell diffusion. This stage in which the systems can be considered as independent shells remains until a second transition temperature T_R involving diffusion of particles between the shells. At higher temperatures, the shell structure disappears. Figure 10 shows the mean crystals (superposition of the different positions of the particles) obtained for instance for $N=18$ at three key temperatures. Figure 10(b) illustrates the role of the transi-

TABLE I. Summary of the different transition temperatures (in 10^{11} K).

N	T_I	T_J	T_O	T_R
18	$T_I < 13$	14	29	$T_R > 30$
19	$T_I > 18$	20	30	$T_R > 30$
20	$13 < T_I < 18$	17	29	$T_R > 30$

tion activity in the loss of the orientational order: according to the values of the angular displacements, particles positions should be distinguishable.

This kind of two-stage “melting” had been suggested by previously cited works, especially in Ref. [14], where the authors focus on a global Lindemann criterion that includes different mechanisms that we have exhibited there. In particular, we have distinguished two contributions in the radial displacements, namely the individual jumps and the mean behavior. In colloidal systems [20,21] the system is arranged at low temperature in a shell-like structure. It also exhibits a very similar behavior when the temperature increases, excepted a re-entrant ordered phase which was not observed in our case, this phase being specific to the hard wall confinement [33].

In Ref. [22], the authors studied the “melting” of $N=19$ and $N=20$ quantum particles interacting with coulombic interaction. They described the “melting” as a two stages process: first an orientational inter and intrashell disordering and then a radial “melting” at higher temperatures. The relative positions of the transition temperatures found here are in good qualitative agreement with their results. In addition, we can clearly distinguish two phases in the angular disordering, namely an intershell rotation and then an intrashell “melting”. This last point is also presented in numerical works on classical coulombic particles [27].

Whereas local geometry have an influence on the configuration transitions through commensurability considerations, we have shown that its effects are neglectable for the intrashell displacements as well as for the radial ones. On the other hand, correlation functions define very different temperatures for our three systems (all the transition temperatures are summarized in Table I). Moreover, and contrary to large systems, those temperatures are lower than the transition temperatures given by the Lindemann criterion. We have then to consider that beyond the well-known Lindemann scenario, there are other sources of disorder, namely the configuration switches.

V. CONCLUSION

In this paper we show that for a system constituted of a small number of interacting particles like Wigner islands, an increase of temperature results in a disordering of the system more than a real melting. This disordering process is very sensitive to the local order of the explored configurations.

This disordering results from both individual excitations that induce configuration transitions and collective excitations. This process is marked by three different transitions.

The temporal correlation functions which describe the correlation loss of the system exhibits an exponential decrease at the “liquid transition temperature” T_l (named after the usual convention). This first transition is identified without ambiguity as corresponding to the increase of configuration transitions between the stable and metastable states of the system. So the liquid transition temperature depends strongly on the local order as the transition rate. At larger temperatures, two other transitions appear, T_O and T_R characterizing, respectively, intrashell and intershell diffusion. These transitions are evidenced by the change of the mean square displacements with temperature and correspond to collective excitations. The local order play a less significant role in the transition temperature values.

This disordering process and the importance of the local order on these temperatures are due the small number of configuration states explored by the system at a fixed temperature. From this point of view, it is a specific characteris-

tic of small systems. Indeed, these effects cannot be observed for large systems since the number of explored configurations is large enough to mask the individual excitations in the collective ones, hence, the coincidence between the transition temperatures described by the correlation functions and those identified by the Lindemann criterion.

Whereas the T_l transition was never discussed before, the two following successive transitions have previously been mentioned in the literature. The corresponding analyses are in agreement with our results but their approach is very different. We show that the description of the transition from well organized arrays towards liquid state resulting from successive excitations requires more detailed analyses than the single use of the Lindemann criterion.

Finally, let us conclude by suggesting that small Wigner islands that we proposed could be good candidates in order to explore experimentally the thermodynamic laws dedicated to small systems of interacting particles [34].

-
- [1] G. Blatter, M. V. Feigel'man, V. B. Geshkenbein, A. I. Larkin, and V. M. Vinokur, *Rev. Mod. Phys.* **66**, 1125 (1994).
- [2] Y. Hata, J. Suzuki, I. Kakeya, K. Kadowaki, A. Odawara, A. Nagata, S. Nakayama, and K. Chinone, *Physica C* **388**, 719 (2003).
- [3] R. Ashoori, *Nature (London)* **379**, 413 (1996).
- [4] J. M. Liu, W. T. Juan, J. W. Hsu, Z. H. Huang, and L. I., *Plasma Phys. Controlled Fusion* **41**, A47 (1999).
- [5] S. L. Gilbert, J. J. Bollinger, and D. J. Wineland, *Phys. Rev. Lett.* **60**, 2022 (1988).
- [6] E. J. Yarmchuck and R. E. Packard, *J. Low Temp. Phys.* **46**, 479 (1982).
- [7] P. Leiderer, W. Ebner, and V. B. Shikin, *Surf. Sci.* **113**, 405 (1982).
- [8] F. Chevy, K. W. Madison, and J. Dalibard, *Phys. Rev. Lett.* **85**, 2223 (2000).
- [9] K. Zahn, R. Lenke, and G. Maret, *Phys. Rev. Lett.* **82**, 2721 (1999).
- [10] M. S. Jean, C. Guthmann, and G. Coupier, *Eur. Phys. J. B* **39**, 61 (2004).
- [11] M. S. Jean, C. Even, and C. Guthmann, *Europhys. Lett.* **55**, 45 (2001).
- [12] M. S. Jean and C. Guthmann, *J. Phys.: Condens. Matter* **14**, 13653 (2002).
- [13] L. J. Campbell and R. M. Ziff, *Phys. Rev. B* **20**, 1886 (1979).
- [14] V. M. Bedanov and F. M. Peeters, *Phys. Rev. B* **49**, 2667 (1994).
- [15] Y. J. Lai and L. I, *Phys. Rev. E* **60**, 4743 (1999).
- [16] V. A. Schweigert and F. M. Peeters, *J. Phys.: Condens. Matter* **10**, 2417 (1998).
- [17] M. Kong, B. Partoens, and F. M. Peeters, *Phys. Rev. E* **65**, 046602 (2002).
- [18] V. A. Schweigert and F. M. Peeters, *Phys. Rev. B* **51**, 7700 (1995).
- [19] B. Partoens and P. S. Deo, *Phys. Rev. B* **69**, 245415 (2004).
- [20] R. Bubeck, C. Bechinger, S. Nesper, and P. Leiderer, *Phys. Rev. Lett.* **82**, 3364 (1999).
- [21] R. Bubeck, P. Leiderer, and C. Bechinger, *Europhys. Lett.* **60**, 474 (2002).
- [22] A. V. Filinov, M. Bonitz, and Y. E. Lozovik, *Phys. Rev. Lett.* **86**, 3851 (2001).
- [23] A. P. Young, *Phys. Rev. B* **19**, 1855 (1979).
- [24] D. R. Nelson and B. I. Halperin, *Phys. Rev. B* **19**, 2457 (1979).
- [25] D. R. Nelson, in *Phase Transition and Critical Phenomena*, edited by C. Domb and J. L. Lebowitz (Academic Press, New York, 1983), Vol. 7.
- [26] K. Zahn and G. Maret, *Phys. Rev. Lett.* **85**, 3656 (2000).
- [27] V. M. Bedanov, G. V. Gadiyak, and Y. E. Lozovik, *Phys. Lett.* **109**, 289 (1985).
- [28] Y. E. Lozovik, V. M. Farztdinov, B. Abdullaev, and S. A. Kucherov, *Phys. Lett.* **112**, 61 (1985).
- [29] V. M. Bedanov, G. V. Gadiyak, and Y. E. Lozovik, *Sov. Phys. JETP* **61**, 967 (1985).
- [30] C. Meyers and M. Daumens, *Phys. Rev. B* **62**, 9762 (2000).
- [31] B. Pouligny, R. Malzbender, P. Ryan, and N. A. Clark, *Phys. Rev. B* **42**, 988 (1990).
- [32] H. A. Kramers, *Physica (Amsterdam)* **7**, 284 (1940).
- [33] I. V. Schweigert, V. A. Schweigert, and F. M. Peeters, *Phys. Rev. Lett.* **84**, 4381 (2000).
- [34] T. Dauxois, S. Ruffo, E. Arimondo, and M. Wilkens, *Dynamics and Thermodynamics of Systems with Long-Range Interactions* (Springer, New York, 2002).